Development 135, 899-908 (2008) doi:10.1242/dev.006742

Oscillatory lunatic fringe activity is crucial for segmentation of the anterior but not posterior skeleton

Emily T. Shifley, Kellie M. VanHorn, Ariadna Perez-Balaguer*, John D. Franklin†, Michael Weinstein and Susan E. Cole‡

The Notch pathway plays multiple roles during vertebrate somitogenesis, functioning in the segmentation clock and during rostral/caudal (R/C) somite patterning. Lunatic fringe (*Lfng*) encodes a glycosyltransferase that modulates Notch signaling, and its expression patterns suggest roles in both of these processes. To dissect the roles played by *Lfng* during somitogenesis, a novel allele was established that lacks cyclic *Lfng* expression within the segmentation clock, but that maintains expression during R/C somite patterning (*Lfng*$^{\Delta FCE1}$). In the absence of oscillatory *Lfng* expression, Notch activation is ubiquitous in the PSM of *Lfng*$^{\Delta FCE1}$ embryos. *Lfng*$^{\Delta FCE1}$ mice exhibit severe segmentation phenotypes in the thoracic and lumbar skeleton. However, the sacral and tail vertebrae are only minimally affected in *Lfng*$^{\Delta FCE1}$ mice, suggesting that oscillatory *Lfng* expression and cyclic Notch activation are important in the segmentation of the thoracic and lumbar axial skeleton (primary body formation), but are largely dispensable for the development of sacral and tail vertebrae (secondary body formation). Furthermore, we find that the loss of cyclic *Lfng* has distinct effects on the expression of other clock genes during these two stages of development. Finally, we find that *Lfng*$^{\Delta FCE1}$ embryos undergo relatively normal R/C somite patterning, confirming that *Lfng* roles in the segmentation clock are distinct from its functions in somite patterning. These results suggest that the segmentation clock may employ varied regulatory mechanisms during distinct stages of anterior/posterior axis development, and uncover previously unappreciated connections between the segmentation clock, and the processes of primary and secondary body formation.

KEY WORDS: Lunatic fringe, Notch, Segmentation clock, Somitogenesis, Secondary body formation, Mouse

INTRODUCTION

The segmentation of the vertebrate embryo is most obvious during the process of somitogenesis. Somites are the embryonic precursors to the axial skeleton, striated muscle and dermis of the back, and are formed by sequential budding from the anterior-most region of the presomitic mesoderm (PSM) (reviewed by Christ et al., 1998; Gossler and Hrabe de Angelis, 1998). This process is dynamic and complex. During gastrulation, cells enter the presomitic mesoderm via the primitive streak. Later in development (~10.0 dpc) the tailbud forms, and further mesodermal cells arise from this structure (Gossler and Tam, 2002). Although this distinction between primary body formation (giving rise to cervical, thoracic and lumbar vertebrae) and secondary body formation (giving rise to post-anal structures) was originally proposed in 1925 (Holmdahl, 1925), it remains unclear how, and to what extent, the genetic regulation of somitogenesis between these two processes may vary (reviewed by Handrigan, 2003).

Several models for the control of somitogenesis invoke a clock that provides a timing mechanism for segmentation (Cooke and Zeeman, 1976; Kerszberg and Wolpert, 2000; Meinhardt, 1986; Schnell and Maini, 2000). These models differ in their specifics, but all include an oscillating activity in the PSM with a period identical to the rate of somite formation. Molecular evidence for the segmentation clock came initially from the cyclic expression pattern of chicken *c-hairy* RNA (Palmeirim et al., 1997). Shortly thereafter, lunatic fringe (*Lfng*) RNA was found to have oscillatory expression patterns in the PSM, linking it to the clock as well (Aulehla and Johnson, 1999; Forsberg et al., 1998; McGrew et al., 1998).

The importance of Notch signaling during vertebrate segmentation is evident from the phenotypes associated with mutations in Notch pathway genes, many of which cause defects in embryonic segmentation. Furthermore, cyclic gene expression has been described in the presomitic mesoderm for many other genes linked to the Notch signaling pathway in mouse, zebrafish and chick (reviewed by Rida et al., 2004; Shifley and Cole, 2007). The Wnt pathway has also been linked to the clock. Both *Axin2* and *Nkd1* RNA levels oscillate in the PSM, and it has been suggested that the Wnt pathway lies upstream of oscillatory Notch signaling (Aulehla et al., 2003; Ishikawa et al., 2004). More recently, a large number of oscillatory genes have been identified, many of which are linked to the Notch, Wnt or FGF pathways (Dequeant et al., 2006), suggesting complex clock regulation involving multiple signaling pathways.

The analysis of Notch signaling in the segmentation clock mechanism is complicated by the fact that this pathway plays multiple roles during somitogenesis. The PSM can be divided into functionally distinct regions based on RNA expression patterns (reviewed by Saga and Takeda, 2001). In the posterior PSM (region I), cyclic expression of several genes reflects the function of the segmentation clock. In the anterior PSM (region II) the expression of the cycling genes is stabilized, and the pre-somites develop rostral and caudal compartments. These regions are demarcated by the graded expression of FGF8 in region I, which has been suggested to maintain the immature state of the cells (Dubrulle et al., 2001; Sawada et al., 2001). Several lines of evidence suggest that Notch signaling plays distinct roles in these two regions. In region I of the PSM, Notch activity levels oscillate, suggesting its function in this region is linked to the clock (Huppert et al., 2005; Morimoto et al., 2005). Some models suggest that this oscillatory activation may be achieved partially through the transitory inhibition of Notch

Department of Molecular Genetics, The Ohio State University, 984 Biological Sciences Building, 484 West 12th Avenue, Columbus, OH 43210-1292, USA.

*Present address: Universidad Miguel Hernandez, Alicante, Spain
†Present address: The University of Toledo, Toledo, OH 43606-3390, USA
‡Author for correspondence (e-mail: cole.354@osu.edu)

Accepted 20 December 2007

signaling via its glycosylation by LFNG in the Golgi, and transcriptional feedback loops involving *Hes7* (Dale et al., 2003). This oscillatory mechanism, however, clearly receives input from other members of the Notch pathway and from other signaling pathways, including Wnt and FGF. This complex network of interlocked oscillatory genes has been proposed to contribute to the robust nature of somitogenesis (Dequeant et al., 2006). Notch signaling also plays crucial roles in the patterning of the presumptive somites in region II of the PSM. It appears that interplay between the Mesp genes and the Notch pathway is required for the establishment of rostrocaudal polarity in the developing somites, with *Mesp2* acting through the Notch pathway to downregulate *Dll1* expression in the presumptive rostral somite compartment, while in the presumptive caudal compartment, Notch signaling upregulates *Dll1* expression. *Lfng* is a direct target of *Mesp2*, and its stable expression in the rostral compartment may inhibit Notch signaling in this compartment (Morimoto et al., 2005; Takahashi et al., 2000).

We and others have defined genomic sequences sufficient to direct cyclic expression of *Lfng* in the PSM, and demonstrated that independent *Lfng* cis-acting regulatory regions drive stable RNA expression in the rostral compartment of the developing somites in the anterior PSM (Cole et al., 2002; Morales et al., 2002). Deletion of a conserved regulatory element termed fringe clock element 1 (FCE1) from *Lfng* reporter transgenes eliminates cyclic expression in the caudal PSM, while maintaining expression in the anterior PSM, reflecting the distinct roles of *Lfng* in the segmentation clock and in R/C patterning of developing somites. Thus, the complex phenotypes of $Lfng^{-/-}$ mice may arise from disruption of both of these roles, with variations in somite size perhaps resulting from impaired clock function, while the apparent mingling of somite compartments might be exacerbated by altered R/C patterning.

To dissect the functions of the Notch pathway during segmentation, we perturbed only one of the roles of Notch signaling, by disrupting oscillatory *Lfng* expression in region I of the PSM, while sparing its expression in region II of the PSM. We report here that the clock and patterning roles of *Lfng* during somitogenesis are functionally separable. Strikingly, we find that the loss of oscillatory *Lfng* expression and Notch1 activity in region I of the PSM has more severe effects during the segmentation of the thoracic and lumbar skeleton than the sacral and tail skeleton. This suggests that oscillatory Notch1 activation in the segmentation clock is much more important during primary body formation than during secondary body formation. By contrast, the specific localization of Notch activity to the presumptive caudal compartment of the presomite in region II of the PSM is important throughout development.

MATERIALS AND METHODS

Targeted deletion of FCE1

FCE1 and minimal flanking sequences were deleted from the *Lfng* fragment extending from the 5′*Xho*I site in the 5′ flank to the *Hin*dIII site in intron 1 and replaced with an *Eco*RV site (final allele: ggacttttttccttgtcctGATATCaccaccatatcccactcc, upper case=*Eco*RV). This deleted fragment was the 5′flanking sequence for a floxed neo/testis cre cassette (Bunting et al., 1999). 3′ flanking sequences extended from the *Hin*dIII site to the *Xho*I site in intron 1. Linearized vector was electroporated into TC1 cells (Deng et al., 1996) and G418 resistant colonies were screened by Southern blot. Two independent ES cell lines were injected by the OSUCCC Transgenic/ES Core Facility, and transmitted through the germline. Results from the lines were identical and are combined. Mice were maintained on a mixed 129/Sv×C57BL/6J background. $Lfng^{tmRjo1/+}$ mice (R. Johnson), were maintained on a mixed 129/Sv×C57BL/6J background, or crossed one generation with FVB/J mice to increase the recovery of adult $Lfng^{tmRjo1/tmRjo1}$ mice (referred to as $Lfng^{-/-}$). Mice were maintained under the care of the Ohio State University ILACUC.

Genotyping

Genomic DNA was prepared from tail clips via proteinase K saltout or from yolk sac fragments via the HOTSHOT procedure (Truett et al., 2000). Animals were genotyped by PCR. $Lfng^{tmRjo1}$ primers FNG322 (5′-GAGCACCAGGAGACAAGCC-3′), FNG325 (5′-AGAGTTCCTGAAGCGAGAG-3′) and PGK3 (5′-CTTGTGTAGCGCCAAGTGC-3′) amplify a 170 bp wild-type product and a 200 bp mutant product. $Lfng^{\Delta FCE1}$ primers SC284 (5′-TTTGGTGGGAATGGATTAGC-3′) and SC285 (5′-CTGGTCCATTTGCTCTGAGG-3′) produce a 340 bp wild-type and a 182 bp mutant bands, while SC286 (5′-TTGGGTCTATCTGGGAAACG-3′) and SC287 (5′-GCGACTCATCCAGACACAGA-3′) produce a 149 bp wild-type and a 250 bp mutant bands.

Whole mount in situ hybridization

Embryos were collected from timed pregnancies (noon of the day of plug identification designated as 0.5 dpc). RNA in situ hybridization using digoxigenin-labeled probes was performed essentially as described (Riddle et al., 1993); however, embryos were blocked in a mixture of MABT +20% sheep serum +2% Boehringer blocking reagent, and all post-antibody washes were performed in MABT. *Hes7* cDNA probes extend from the internal *Sma*I site to the stop codon. *Hes7* intron probe was amplified using the primers 5′-GCTAGAGGCCATAGCTGGTG and 5′-CTGTGACCAGCGGGAAAG. *Dll1* intron probe was amplified using primers 5′-GTTGGCAGTGGGAAGAAGG and 5′-TGTGTTGTGCCAATGAAGGT. *Nrarp* probe was amplified using the primers 5′-GCGTGGTTATGGGAGAAAGA and 5′-TTCCTCCCACACTGGTTCAT. The *Hesr1* probe comprises the coding region of the cDNA. Other probes were *Lfng* (Johnston et al., 1997), *Mesp2* (Saga et al., 1997), *Uncx4.1* (Mansouri et al., 1997) and *Mox2* (Candia et al., 1992).

Skeletal preparations, neurofilament staining and histology

Skeletal preparations of neonates or 18.5 dpc embryos were performed essentially as described (Kessel and Gruss, 1991). Neurofilament staining was performed using the 2H3 antibody (Developmental Studies Hybridoma Bank), using standard protocols. For histological analysis, embryos were fixed in Bouin's fixative and transferred to ethanol for storage. Embryos were embedded in paraffin and 10 μm sections were stained with Haemotoxylin and Eosin.

Whole mount immunohistochemistry

Embryos were fixed in fresh 4% PFA in PBS, then washed in PBS. After overnight incubation at 4°C in PBS containing 0.1% hydrogen peroxide, 1% Triton X-100 and 10% fetal calf serum (TS-PBS), embryos were transferred into 10 mM sodium citrate (pH 6.0), 0.1% Tween-20 (CT), boiled for 10 minutes and then transferred back to PBS. After washing in TS-PBS, embryos were incubated for 5 days in primary Cleaved Notch1 (Val1744) antibody (Cell Signaling Technology) in TS-PBS (1:250). After washing embryos were incubated overnight in AP-conjugated secondary antibody in MABT (1:500). After washing, embryos were transferred to NTMT and stained with BCIP/NBT as described (Riddle et al., 1993).

RESULTS

Deletion of FCE1 from the *Lfng* locus perturbs clock-linked *Lfng* RNA expression

To specifically disrupt *Lfng* expression in the segmentation clock, we deleted FCE1 from the endogenous *Lfng* locus producing the allele $Lfng^{\Delta FCE1}$ (Fig. 1A,B). We hypothesized that this mutation would disrupt expression of *Lfng* in the caudal PSM (region I), where the clock is active, while preserving *Lfng* expression in the anterior PSM (region II), where R/C somite patterning is initiated.

Lfng expression is perturbed in the PSM of $Lfng^{\Delta FCE1/\Delta FCE1}$ mutant embryos. In wild-type embryos, three distinct phases of *Lfng* expression are seen in the PSM, reflecting cyclic expression (Fig. 1C, parts c-f). By contrast, $Lfng^{\Delta FCE1/\Delta FCE1}$ embryos express *Lfng* RNA in a single band in the anterior PSM, with no expression observed in the caudal PSM where the clock is active (Fig. 1C, parts g,h). Similar results were seen at stages between 8.5 and 11.5 dpc

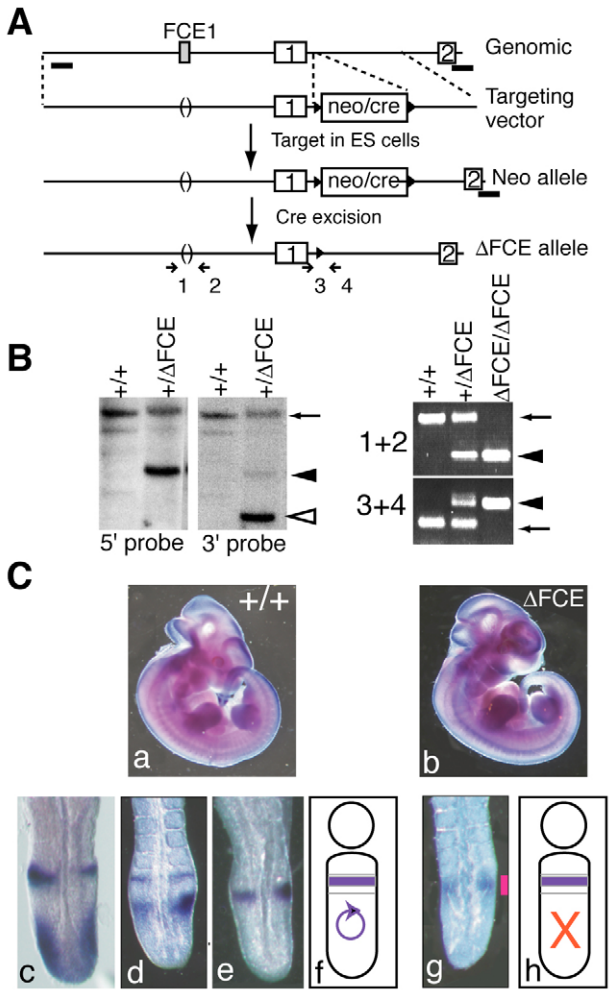

Fig. 1. Deletion of FCE1 from the endogenous locus alters *Lfng* expression in the posterior PSM. (**A**) The *Lfng* endogenous locus (boxes signify coding exons and FCE1), the targeting vector replacing the 110 bp FCE1 sequence with an *Eco*RV site and the structure of the targeted locus are shown. The floxed Neo/Testis-CRE cassette is excised upon passage through the male germline (Bunting et al., 1999). Locations of probes (solid lines) and primers (numbered arrows) used for genotyping are indicated. (**B**) After electroporation into TC1 cells (Deng et al., 1996), G418 resistant colonies were screened by Southern blot. A representative colony containing the $Lfng^{\Delta FCE1}$ allele and a mouse genotyping PCR are shown. Arrows, endogenous band; arrowheads, targeted bands. (**C**) RNA in situ analysis demonstrates cyclic *Lfng* expression in wild-type embryos at 10.5 dpc (c-e, *n*=4/14 Phase 1, 5/14 Phase 2, 5/14 Phase 3). In homozygous mutant embryos, expression is seen only in the anterior PSM (g, *n*=11). PSM expression patterns are summarized (f,h). *Lfng* RNA expression at other sites is unaffected (a,b).

(data not shown). Although the anterior band of *Lfng* expression in $Lfng^{\Delta FCE1/\Delta FCE1}$ embryos is weaker than the anterior-most band of *Lfng* expression in wild-type embryos, these results demonstrate that the deletion of the FCE1 enhancer prevents oscillatory expression of *Lfng* in region I of the PSM, while sparing some level of expression in region II. In addition, we find that *Lfng* expression in region II of the PSM is largely confined to the presumptive rostral compartment of somite S-1 (data not shown), indicating that the endogenous *Lfng* expression pattern in the anterior PSM is preserved in the $Lfng^{\Delta FCE1}$ allele.

The loss of *Lfng* expression in the segmentation clock perturbs normal skeletal development

Although the $Lfng^{-/-}$ genotype is reported to be viable, we find that on a mixed 129/Sv×C57BL/6J background, only rare animals survive postnatally, and homozygous males are infertile. By contrast, homozygous $Lfng^{\Delta FCE1/\Delta FCE1}$ animals survive to adulthood at Mendelian ratios, and homozygous animals of both sexes are fertile. $Lfng^{\Delta FCE1/\Delta FCE1}$ animals have segmentation defects, including shortened body and variably kinked tails (Fig. 2A). In the anterior skeleton, both $Lfng^{-/-}$ and $Lfng^{\Delta FCE1/\Delta FCE1}$ animals are severely affected. Multiple rib fusions and bifurcations as well as severely disorganized vertebrae are observed (Fig. 2B). When defects in the thoracic region of the skeleton are quantified, we find similar levels of disorganization in $Lfng^{\Delta FCE1/\Delta FCE1}$ and $Lfng^{-/-}$ animals (Fig. 2C).

In the more posterior skeleton, however, $Lfng^{\Delta FCE1/\Delta FCE1}$ animals are much less affected than $Lfng^{-/-}$ animals (Fig. 2B,D). In the thoracic and lumbar region of the skeleton, vertebral condensations in both $Lfng^{\Delta FCE1/\Delta FCE1}$ and $Lfng^{-/-}$ animals are irregular and misaligned. Strikingly, this pattern is altered at the lumbo-sacral junction. In the sacral region of $Lfng^{\Delta FCE1/\Delta FCE1}$ animals, normal vertebral condensations are seen in all animals, and the tail vertebrae appear relatively normal, though variable kinks in the tail are seen ranging from mild (0-1 in 40% of mice) to moderate (2-5 in 60% of mice). By contrast, in $Lfng^{-/-}$ animals, vertebral condensations are abnormal throughout the sacral region and the tail appears truncated, a phenotype never seen in $Lfng^{\Delta FCE1/\Delta FCE1}$ animals (Fig. 2B,D). Thus we find that the loss of oscillatory *Lfng* expression in region I of the PSM causes pronounced defects in the axial skeleton, but these defects are much more pronounced in the thoracic and lumbar regions, while the sacral and more caudal regions of the skeleton are less affected in comparison to the null allele. Interestingly, the lumbo-sacral junction, the point where skeletal morphology largely recovers in $Lfng^{\Delta FCE1/\Delta FCE1}$ animals, represents the transition point between primary and secondary body formation, suggesting that oscillatory *Lfng* plays, at most, a minor role in secondary body formation.

The $Lfng^{\Delta FCE1}$ allele affects somite formation differently during primary and secondary body formation

To test the hypothesis that early and late somitogenesis are differentially affected by the loss of oscillatory Lfng expression, we examined somite morphology at different stages of embryonic development. Somites that contribute to the thoracic and lumbar regions of the skeleton are produced during primary body formation (Gossler and Tam, 2002). In $Lfng^{\Delta FCE1/\Delta FCE1}$ embryos, these somites are irregularly sized and spaced with frequent fusions between neighboring somites (Fig. 3B), and the mature derivatives of these somites remain irregularly spaced and sized at 10.5 dpc (Fig. 3D). During secondary body formation, however, somite development recovers in $Lfng^{\Delta FCE1/\Delta FCE1}$ embryos, producing relatively evenly sized and spaced epithelial somites (Fig. 3F). These data support the idea that the loss of oscillatory *Lfng* expression differentially affects primary and secondary body formation with thoracic and lumbar somites being more sensitive to the loss of cyclic *Lfng* activity than are more caudal somites.

Rostral-caudal somite patterning is partially rescued in $Lfng^{\Delta FCE1/\Delta FCE1}$ embryos

$Lfng^{-/-}$ embryos have severe defects in R/C somite patterning (Evrard et al., 1998; Zhang and Gridley, 1998). To address whether the *Lfng* expression in region II of the PSM of $Lfng^{\Delta FCE1/\Delta FCE1}$ embryos could rescue R/C patterning, we examined compartment

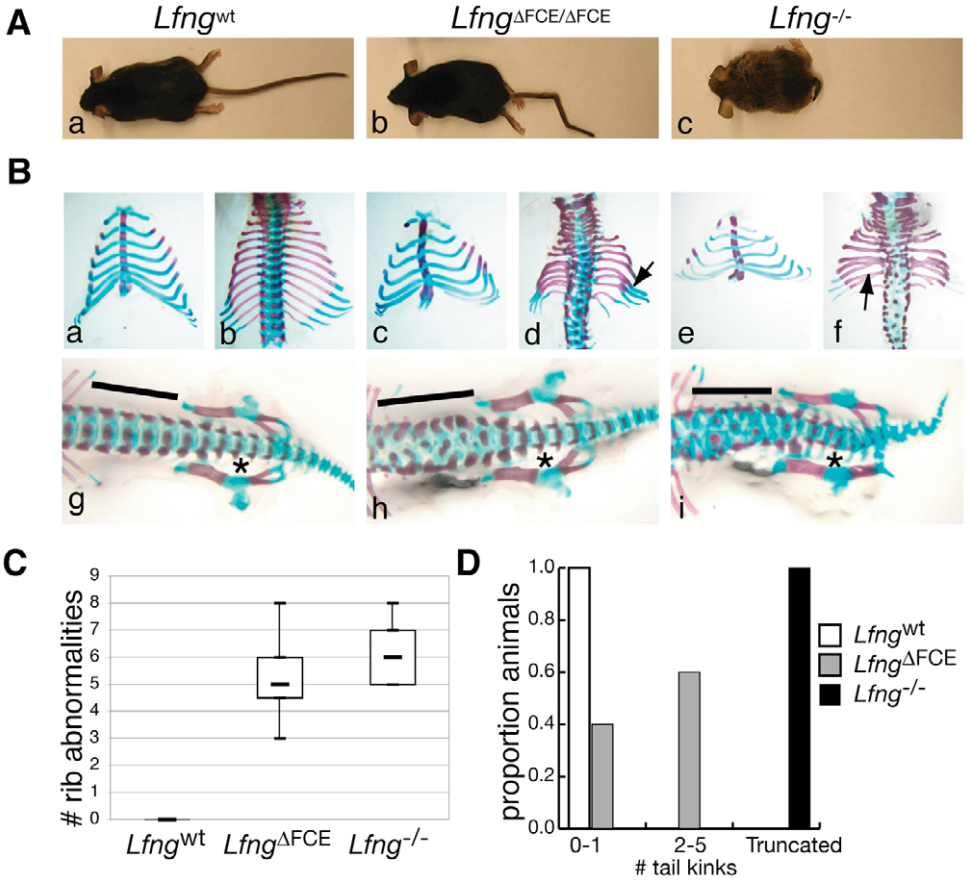

Fig. 2. The *Lfng*$^{\Delta FCE1}$ allele interferes with normal skeletal development during primary body formation. (**A**) Representative phenotypes of *Lfng*$^{+/-}$, *Lfng*$^{\Delta FCE1/\Delta FCE1}$ and *Lfng*$^{-/-}$ mice. The *Lfng*$^{\Delta FCE1/\Delta FCE1}$ mouse has a shortened body and kinked tail. (**B**) Skeletal preparations of wild-type (a,b,g), *Lfng*$^{\Delta FCE1/\Delta FCE1}$ (c,d,h) and *Lfng*$^{-/-}$ (e,f,i) mice. Ventral (a,c,e) and dorsal (b,d,f) views of the ribs and dorsal views of the lumbar and sacral spine (g-i) are shown. The thoracic regions of *Lfng*$^{\Delta FCE1/\Delta FCE1}$ (c,d) and *Lfng*$^{-/-}$ (e,f) mice exhibit rib fusions (arrows) and disorganized vertebrae. In *Lfng*$^{\Delta FCE1/\Delta FCE1}$ skeletons, vertebral disorganization extends through the lumbar region (bar, h), but normal vertebral condensations are seen in the sacral spine (*). By contrast, vertebral disorganization extends throughout the lumbar (bar) and sacral (*) regions of *Lfng*$^{-/-}$ skeletons (i), and the tail appears severely truncated. (**C**) Rib abnormalities were quantified in *Lfng* wild-type (n=17), *Lfng*$^{\Delta FCE1/\Delta FCE1}$ (n=11) and *Lfng*$^{-/-}$ (n=8) neonates. Results are shown as bar and whisker graphs (solid horizontal line indicates the mean), with the number of rib abnormalities indicated on the y-axis. The number of rib abnormalities is similar in *Lfng*$^{-/-}$ and *Lfng*$^{\Delta FCE1/\Delta FCE1}$ animals (P=0.236, the null hypothesis is accepted). (**D**) Tail anomalies were quantified in adult animals. The proportion of animals with 0-1 kinks, 2-5 kinks or truncated tails are shown. Forty percent of *Lfng*$^{\Delta FCE1/\Delta FCE1}$ animals exhibit mild tail defects (0-1 kinks), while the remaining animals had between 2 and 5 kinks. By contrast, *Lfng*$^{-/-}$ animals exhibit truncation in the tail region.

formation in the anterior PSM and in mature somites of *Lfng* mutant mice. We examined R/C patterning in region II of the PSM by assessing the expression of *Mesp2*. *Mesp2* defines the presumptive rostral compartment of somite S-1, and interacts with *Lfng* and Notch1 signaling during the process of R/C patterning (Morimoto et al., 2005; Takahashi et al., 2000). During both primary and secondary body formation, we find that *Mesp2* is expressed in a single band of varying width in the anterior PSM of both wild-type and *Lfng*$^{\Delta FCE1/\Delta FCE1}$ embryos, reflecting the early expression and subsequent refinement of *Mesp2* in the presumptive rostral compartment. However, in *Lfng*$^{\Delta FCE1/\Delta FCE1}$ embryos, we frequently see a less distinct rostral border, regardless of the stage of somitogenesis (Fig. 4A). These results demonstrate that the rostral compartment is being defined in the presomites in region II of *Lfng*$^{\Delta FCE1/\Delta FCE1}$ embryos throughout somitogenesis but may suggest that this earliest marker of patterning is mildly disrupted. As this disruption is seen throughout somitogenesis, it may be due to the reduced dose of *Lfng* in the anterior PSM, rather than to differences in primary and secondary body formation.

We then examined patterning of the mature somites. *Uncx4.1*, marking the caudal compartment of epithelial and mature somites, is expressed in clear compartments in all somites of wild-type embryos during primary body formation (Fig. 4B, parts a,b). In *Lfng*$^{-/-}$ embryos, little compartmentalization of somites is seen, with rostral and caudal cells appearing mixed in a ‘salt and pepper’ pattern (Fig. 4B, parts i,j) (Evrard et al., 1998; Zhang and Gridley, 1998). In *Lfng*$^{\Delta FCE1/\Delta FCE1}$ embryos, *Uncx4.1* expression in newly formed somites is largely compartmentalized, with stronger expression in the more caudal region of somites S1 and S2. Clearer compartmentalization is observed in more anterior somites, but compartments are frequently irregularly spaced (Fig. 4B, parts e,f). Compartmentalization of mature somites in the thoracic region of *Lfng*$^{\Delta FCE1/\Delta FCE1}$ embryos is more distinct by 10.5 dpc, with clear bands of *Uncx4.1* visible in the sclerotome. Again, compartments of *Uncx4.1* expression are frequently irregularly spaced or shaped, presumably reflecting the irregularities in somite size and shape observed morphologically in the thoracic region of the embryo (Fig. 4B, part g). Similar results are seen when examining *Mox1* at 10.5 dpc (Fig. 4C). By contrast, the *Uncx4.1* signal in the thoracic region of *Lfng*$^{-/-}$ embryos fails to compartmentalize, maintaining an unsegmented pattern (Fig. 4B, part k). The somites formed during secondary body formation in *Lfng*$^{\Delta FCE1/\Delta FCE1}$ embryos are clearly compartmentalized with regular rostral and caudal segmentation, whereas in *Lfng*$^{-/-}$ embryos, R/C patterning continues to be abnormal (Fig. 4B, parts h,l).

Functionality of R/C patterning was assessed by neurofilament staining with 2H3. In wild-type embryos, regular neurofilament staining is observed, representing the axonal trajectories of spinal neurons through the rostral somite compartment. In *Lfng*$^{\Delta FCE1/\Delta FCE1}$ embryos, axonal projections are seen, but their spacing is irregular (Fig. 4D). Thus, although *Lfng*$^{\Delta FCE1/\Delta FCE1}$ embryos produce irregular somites during primary body formation, the retention of

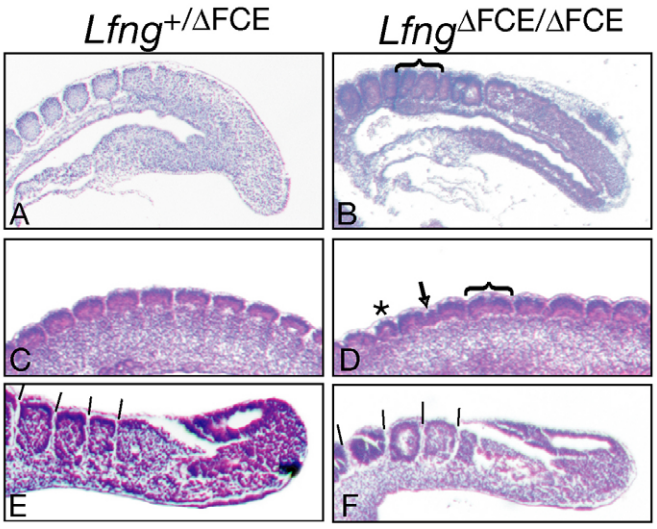

Fig. 3. Early somitogenesis is perturbed in *Lfng*$^{\Delta FCE1/\Delta FCE1}$ embryos. Parasagittal sections of *Lfng*$^{+/\Delta FCE1}$ and *Lfng*$^{\Delta FCE1/\Delta FCE1}$ embryos at 9.5 dpc (**A**,**B**) and 10.5 dpc (**C-F**). At 9.5 dpc, recently formed somites are irregularly sized and shaped in *Lfng*$^{\Delta FCE1/\Delta FCE1}$ embryos (bracket, B). At 10.5 dpc, mature somites in the thoracic region remain irregular in *Lfng*$^{\Delta FCE1/\Delta FCE1}$ embryos with fused (arrow), small (*) and large (bracket) somites seen (D). At this stage, however, the recently formed somites appear relatively normal in wild-type and *Lfng*$^{\Delta FCE1/\Delta FCE1}$ embryos (E,F; lines represent intersomitic boundaries). Anterior is towards the left.

Lfng expression in the anterior PSM supports relatively normal R/C patterning, and somites formed during secondary body formation undergo normal R/C patterning. This supports the idea that the role of *Lfng* in R/C somite patterning is distinct and separable from its functions in the segmentation clock.

The loss of cyclic *Lfng* expression in the posterior PSM perturbs oscillatory NOTCH1 activity

Several groups have suggested that oscillatory expression of *Lfng* is involved in interlocking feedback loops that regulate oscillatory Notch1 activation in the PSM. To examine the effects of the *Lfng*$^{\Delta FCE1}$ allele on Notch1 signaling, we visualized Notch activation using an antibody specific for the Notch1 ICD (NICD). Notch signaling levels oscillate in the PSM of wild-type embryos during primary and secondary body formation (Fig. 5) (Morimoto et al., 2005), with different patterns of NICD staining found in different embryos. By contrast, in both *Lfng*$^{\Delta FCE1/\Delta FCE1}$ (Fig. 5) and *Lfng*$^{-/-}$ (Fig. 5) (Morimoto et al., 2005) embryos, a gradient of NICD is seen in the PSM, reflecting ubiquitous, non-oscillatory Notch signaling throughout the PSM. This confirms that the *Lfng*$^{\Delta FCE1}$ allele inhibits oscillatory Notch signaling in region I of the PSM during both primary and secondary body formation, and indicates that oscillatory Notch activation in region I of the PSM is largely dispensable for segmentation during secondary body formation.

Expression of oscillatory genes is differentially affected during primary and secondary body formation in *Lfng*$^{\Delta FCE1/\Delta FCE1}$ embryos

To assess the effects of the loss of cyclic *Lfng* expression on the transcription of other segmentation clock genes, we first examined the expression of *Hes7* in *Lfng*$^{\Delta FCE1/\Delta FCE1}$ embryos. *Hes7* has been proposed to play a role in the segmentation clock mechanism as part of the feedback loops regulating oscillatory *Lfng* transcription and Notch1 activation (reviewed by Rida et al., 2004). One report has suggested that *Hes7* expression is ubiquitous in the *Lfng*$^{tm1Grid/tm1Grid}$ null background at 9.5 dpc (Chen et al., 2005), while more recent results suggest the *Hes7* expression is affected but still dynamic in the absence of *Lfng* (Niwa et al., 2007). During primary body formation, we used a probe specific for *Hes7* intronic sequences to show that *Hes7* RNA is transcribed in a stable ubiquitous pattern in the PSMs of *Lfng*$^{\Delta FCE1/\Delta FCE1}$ and *Lfng*$^{-/-}$ embryos, distinct from the dynamic banding pattern seen in wild-type embryos (Fig. 6A). Thus, during primary body formation, the loss of *Lfng* prevents the cyclic transcription of *Hes7*. In sharp contrast, we find that during secondary body formation, *Hes7* transcription oscillates in the same way as wild-type expression patterns in both *Lfng*$^{\Delta FCE1/\Delta FCE1}$ and *Lfng*$^{-/-}$ embryos (Fig. 6B). Similar results were seen using a *Hes7* mRNA probe, indicating that post-transcriptional regulation of *Hes7* mRNA levels is also normal in these embryos (Fig. 6C). *Hes7* cyclic expression was confirmed by half tail culture experiments. PSMs were bisected, with one half fixed immediately and the other half cultured before fixation. After 1 hour of culture, the *Hes7* expression pattern in the cultured half is different from the uncultured half regardless of genotype (Fig. 6D). These results suggest that *Hes7* transcription may be differentially controlled during different stages of somitogenesis, requiring Notch oscillations during primary body formation, but not during secondary body formation.

We confirmed and extended these observations by analyzing the expression of other oscillatory genes in *Lfng*$^{\Delta FCE1/\Delta FCE1}$ embryos. Similar to our results with *Hes7*, we find that *Nrarp* expression is differentially affected during primary and secondary body formation. Before tailbud formation, distinctive banding patterns are observed in wild-type, but not in *Lfng*$^{\Delta FCE1/\Delta FCE1}$ embryos (Fig. 7A). After tailbud formation, oscillatory *Nrarp* expression recovers in *Lfng*$^{\Delta FCE1/\Delta FCE1}$ embryos, although the cyclic expression patterns are less distinct than those in wild-type embryos. Other Notch pathway genes also oscillate during secondary body formation in *Lfng*$^{\Delta FCE1/\Delta FCE1}$ embryos, including *Dll1* (Fig. 7B), but the expression of some Notch targets, including *Hesr1* is perturbed at this stage (Fig. 7C). Thus, although multiple genes that may be involved in the segmentation clock mechanism exhibit oscillatory expression in the absence of cyclic Notch activation during secondary body formation in *Lfng*$^{\Delta FCE1/\Delta FCE1}$ embryos, cyclic Notch1 activity is required for proper expression of some genes in the region at this stage.

DISCUSSION

The FCE1 enhancer is necessary for cyclic expression of *Lfng* in region I of the PSM

Ascertaining the functions of Notch signaling in segmentation is complicated by the fact that the pathway plays multiple roles during somitogenesis. It is unclear what aspects of the *Lfng*$^{-/-}$ phenotype can be ascribed to its role in R/C patterning as opposed to any role in clock function, as both aspects of expression are perturbed throughout development in the mouse knockout. Indeed, in zebrafish, *Lfng* is expressed solely in the anterior-most region of the PSM, indicating that in this organism *Lfng* plays no role in the segmentation clock (Prince et al., 2001). We therefore specifically disrupted the oscillatory expression of *Lfng* in region I of the PSM to examine the role it plays in the segmentation clock during mouse somitogenesis. Targeted deletion of FCE1 sequences eliminates expression of *Lfng* in the posterior region of the PSM, indicating that

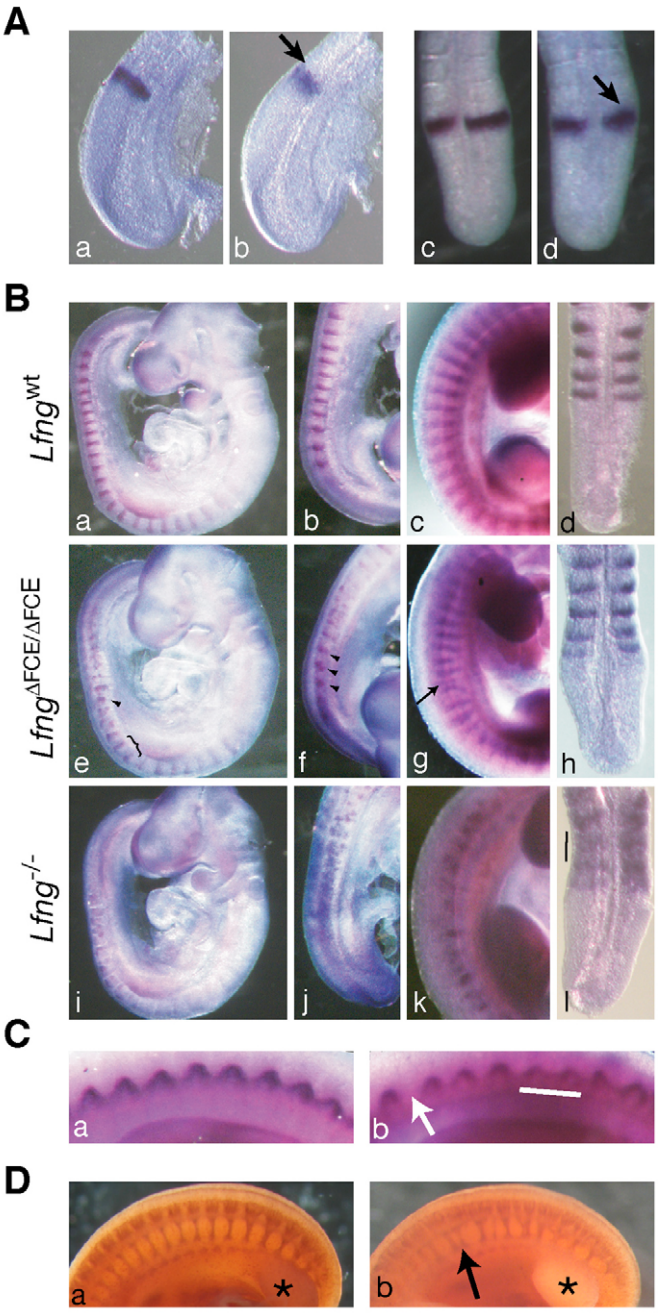

Fig. 4. R/C patterning in *Lfng*$^{\Delta FCE1/\Delta FCE1}$ embryos. (**A**) Whole-mount in situ hybridization for *Mesp2*, defining the presumptive rostral compartment of the pre-somite. In wild-type (a,c) and *Lfng*$^{\Delta FCE1/\Delta FCE1}$ (b,d) embryos, a single clear band of *Mesp2* expression is seen at both 9.0 (a,b) and 10.5 (c,d). The anterior border of this band is sometimes less defined in *Lfng*$^{\Delta FCE1/\Delta FCE1}$ embryos (arrows). (**B**) Whole-mount in situ hybridization with a probe against *Uncx4.1*, which demarcates the caudal half of the somites. At 9.5 and 10.5 dpc, wild-type somites have clear rostral and caudal compartments (a-d). During primary body formation, *Lfng*$^{\Delta FCE1/\Delta FCE1}$ embryos exhibit some compartmentalization with stronger staining in the caudal region of the somite (e,f, arrowheads), although compartments are frequently irregular (e, bracket). At this stage, little compartmentalization in seen in *Lfng*$^{-/-}$ embryos (i,j). The mature derivatives of these somites are patterned; clear rostral compartments are observed in *Lfng*$^{\Delta FCE1/\Delta FCE1}$ embryos in the sclerotome of mature somites in the thoracic region, but compartments may be misshapen or irregularly spaced (arrow, g). Somites in the thoracic region of *Lfng*$^{-/-}$ embryos exhibit no compartmentalization at this stage (k). During secondary body formation, somites in *Lfng*$^{\Delta FCE1/\Delta FCE1}$ embryos are of regular size and are correctly patterned (h), while in *Lfng*$^{-/-}$ embryos at this stage, little to no compartmentalization is observed (bar, l). (**C**) Whole-mount in situ analysis of *Mox1* mRNA demonstrates a regular pattern of mature somitic derivatives in the thoracic region of wild-type embryos at 10.5 dpc. (a) In *Lfng*$^{\Delta FCE1/\Delta FCE1}$ embryos, somitic derivatives in this region are distinct but irregularly spaced (b, arrow, bar). (**D**) Staining with 2H3 reveals the regular pattern of axon projections in the trunk region of wild-type embryos at 10.5 dpc (a). In *Lfng*$^{\Delta FCE1/\Delta FCE1}$ embryos, these projections are spaced irregularly (b, arrow). Anterior is towards the left in all panels. *Hindlimb bud.

the enhancer is required for cyclic *Lfng* transcription in region I of the PSM. However, the anterior band of *Lfng* expression in *Lfng*$^{\Delta FCE1/\Delta FCE1}$ embryos is weaker than that seen in wild-type embryos, perhaps supporting an additional role for FCE1 in enhancing expression of *Lfng* in the anterior PSM.

Oscillatory *Lfng* expression and Notch signaling are crucial for the proper segmentation during primary, but not secondary, body formation

As predicted, the loss of oscillatory *Lfng* expression in region I of the PSM affects segmentation in *Lfng*$^{\Delta FCE1/\Delta FCE1}$ embryos, but distinct effects are seen during primary and secondary body formation. In the thoracic and lumbar skeleton, malformed vertebral condensations and rib abnormalities were seen in *Lfng*$^{\Delta FCE1/\Delta FCE1}$ skeletons (Fig. 2B). The appearance of the vertebrae resembles the phenotypes seen in some cases of autosomal recessive spondylocostal dysostosis caused by mutations in *DLL3* or *LFNG*; both the thoracic and lumbar spine are affected and vertebral bodies are irregularly shaped and fitted together (Bulman et al., 2000; Sparrow et al., 2006). To our surprise, we found that the caudal skeletal regions (sacral and tail vertebrae) were invariably less severely affected in *Lfng*$^{\Delta FCE1/\Delta FCE1}$ animals than in *Lfng*$^{-/-}$ animals. Especially striking is the fact that in the sacral region of the spine, *Lfng*$^{\Delta FCE1/\Delta FCE1}$ animals exhibit essentially normal vertebral formation, whereas irregularities are still seen at this level in *Lfng*$^{-/-}$ skeletons. The point of phenotype recovery at the lumbo-sacral junction indicates that secondary body formation occurs relatively normally in *Lfng*$^{\Delta FCE1/\Delta FCE1}$ embryos.

This differential severity is reflected in the process of somitogenesis throughout development. During primary body formation, somites are frequently abnormal in *Lfng*$^{\Delta FCE1/\Delta FCE1}$ embryos (Fig. 3). The production of irregularly sized somites suggests that the loss of oscillatory *Lfng* expression in region I of the PSM interferes with segmentation clock function during primary body formation. By contrast, during secondary body formation, somites formed in *Lfng*$^{\Delta FCE1/\Delta FCE1}$ embryos are evenly spaced and of regular size, and the phenotypes in the sacral and caudal skeleton are correspondingly milder (Figs 2 and 3). Thus, our data suggest that segmentation of the embryo during primary body formation (contributing to the thoracic and lumbar skeleton) is more sensitive to the loss of cyclic *Lfng* expression than is segmentation during secondary body formation. This sheds new light on one of the classical issues of developmental biology: the extent to which primary and secondary body formation represent distinct mechanisms of development.

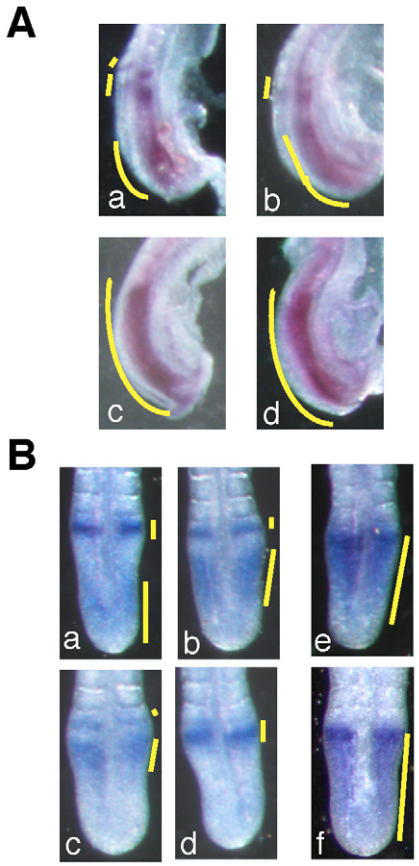

Fig. 5. Notch1 signaling is altered in *Lfng*$^{\Delta FCE1/\Delta FCE1}$ embryos. Whole-mount immunohistochemistry using an antibody specific for activated Notch1 was performed. (**A**) At 8.5 dpc, dynamic domains of Notch activation are seen in wild-type embryos, with anterior bands and a posterior band of varying width (a,b, *n*=29). In both *Lfng*$^{\Delta FCE1/\Delta FCE1}$ (c, *n*=12) and *Lfng*$^{-/-}$ (d, *n*=7) embryos, Notch1 activation is seen ubiquitously throughout the PSM. (**B**) At 10.5 dpc, dynamic Notch1 activation is observed in wild-type embryos, with four distinct phases observed [a-d *n*=9/38 Phase 1, 8/38 Phase 2, 11/38 Phase 3 and 10/38 Phase 4, as defined in Morimoto et al. (Morimoto et al., 2005)]. By contrast, *Lfng*$^{\Delta FCE1/\Delta FCE1}$ (e, *n*=17) and *Lfng*$^{-/-}$ (f, *n*=8) embryos exhibit a gradient of Notch1 activation throughout the PSM. Yellow bars indicate the extent of the stained regions.

Dll3-null embryos exhibit similar *Lfng* expression patterns to those observed in *Lfng*$^{\Delta FCE1/\Delta FCE1}$ mice, with expression observed only in the anterior PSM after 9.5 dpc (Dunwoodie et al., 2002; Kusumi et al., 2004). Interestingly, *Dll3*-null mice exhibit disordered somitogenesis along the length of the vertebral column, suggesting that *Lfng* expression in region II of the PSM is not, in and of itself, sufficient to rescue secondary body formation. This may reflect a requirement for *Dll3* expression in the anterior PSM during secondary body formation. Alternatively, it was recently shown that the loss of *Dll3* in the PSM leads to a loss or reduction in NICD levels in region I of the PSM, in contrast to the ubiquitous Notch1 activation observed in *Lfng*$^{\Delta FCE1/\Delta FCE1}$ embryos (Geffers et al., 2007). This raises the possibility that while oscillatory Notch1 activation in the posterior PSM is not required during secondary body formation, some level of Notch1 activation is still necessary during this process. This may be especially interesting in light of the observation that constitutive overexpression of *Lfng* in the mouse PSM, which might be predicted to repress Notch1 activation, also perturbs somitogenesis along the entire axial skeleton (Serth et al., 2003).

Lfng plays separable roles in the segmentation clock and R/C patterning

Lfng$^{-/-}$ embryos have severe defects in R/C somite patterning (Evrard et al., 1998; Zhang and Gridley, 1998). This could arise due to downstream effects of the loss of *Lfng* in the segmentation clock, or more directly due to the loss of *Lfng* expression in region II of the PSM. Analysis of R/C patterning in *Lfng*$^{\Delta FCE1/\Delta FCE1}$ embryos directly assesses whether the retention of *Lfng* expression in the presumptive anterior compartment of the forming somite can rescue R/C patterning in the absence of oscillatory Notch activity in the clock. During secondary body formation, *Lfng*$^{\Delta FCE1/\Delta FCE1}$ embryos produce regular pairs of somites, and these somites are properly patterned. More surprisingly, the irregular somites produced during primary body formation in *Lfng*$^{\Delta FCE1/\Delta FCE1}$ embryos are also patterned into clear rostral and caudal compartments (Fig. 4B), although this patterning may be somewhat delayed. We propose that in *Lfng*$^{\Delta FCE1/\Delta FCE1}$ embryos, *Mesp2* expression in the anterior compartment of the developing somite is able to stabilize the pattern of Notch activation in somites S0 and S-1, at least in part via its specific activation of *Lfng* transcription. This allows the Notch pathway to function in R/C patterning in *Lfng*$^{\Delta FCE1/\Delta FCE1}$ embryos despite the loss of cyclic *Lfng* expression in region I of the PSM. It is not clear at this time whether the delay in robust R/C patterning of thoracic somites is due to some underlying disorganization of somites S-1 and S0 as a result of perturbed clock function, or whether it may be a result of the reduced *Lfng* levels seen in the anterior PSM in *Lfng*$^{\Delta FCE1/\Delta FCE1}$ embryos. However, the successful patterning of irregularly sized somites during primary body formation in *Lfng*$^{\Delta FCE1/\Delta FCE1}$ embryos suggests that the Notch-based processes involved in the segmentation clock can be largely divorced from its roles in R/C somite patterning, and that the processes regulated by oscillatory Notch signaling in region I of the PSM are not prerequisites for the patterning of the pre-somites in region II.

Differential segmentation clock regulation at distinct levels of the axial skeleton?

The loss of cyclic Notch1 activation has distinct effects during primary and secondary body formation. During early stages of somitogenesis, the loss of oscillatory *Lfng* expression interferes with oscillatory Notch activation (Fig. 5A) and causes phenotypes (irregular somite size and positioning, alteration of oscillatory gene expression) that suggest defects in segmentation clock function (Fig. 3, Fig. 6A). By contrast, during later stages of segmentation, despite the continued absence of oscillatory *Lfng* and the presence of ubiquitous Notch1 activation, somitogenesis proceeds relatively normally in *Lfng*$^{\Delta FCE1/\Delta FCE1}$ embryos, and the oscillatory expression of several clock genes largely recovers at these stages (Fig. 6B-D, Fig. 7). Although expression of some Notch target genes is slightly affected during secondary body formation in *Lfng*$^{\Delta FCE1/\Delta FCE1}$ embryos, the mild phenotypes observed in the caudal axial skeleton suggest that these perturbations are relatively unimportant. Thus, it appears that segmentation clock function is more sensitive to the loss of oscillatory *Lfng* expression during primary body formation than during secondary body formation.

Differential regulation of somitogenesis at different axial levels of the embryo is not unprecedented. The first five or six somites are frequently spared in mutations that affect the Notch signaling

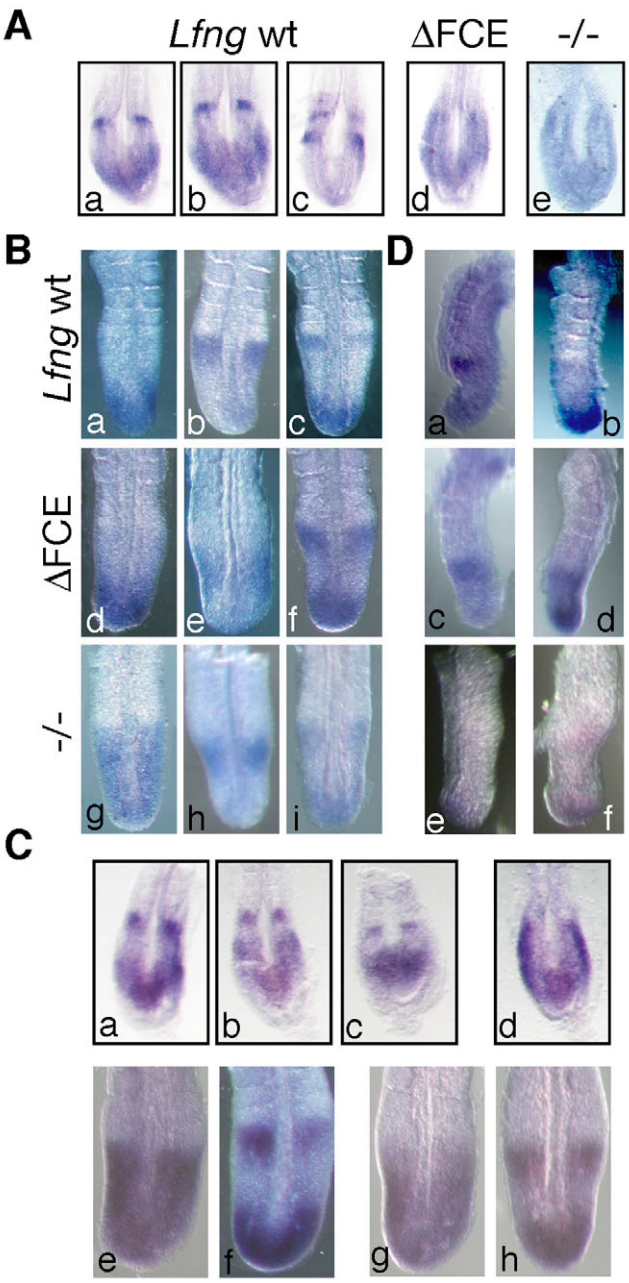

Fig. 6. *Hes7* transcription is affected in *Lfng*$^{\Delta FCE1/\Delta FCE1}$ embryos. (**A**) *Hes7* expression in 8.5 dpc embryos, using a probe specific for intronic sequences. In wild-type embryos, several distinct patterns of expression are seen with a *Hes7* intron probe (a-c, *n*=20), reflecting cyclic *Hes7* transcription. In *Lfng*$^{\Delta FCE1/\Delta FCE1}$ (d, *n*=6) or *Lfng*$^{-/-}$ (e, *n*=4) embryos, *Hes7* mRNA is transcribed ubiquitously throughout the PSM, suggesting that, at this stage, *Lfng* activity is required for *Hes7* oscillation. (**B**) *Hes7* expression, as detected with a probe specific for intronic sequences in 10.5 dpc embryos. At 10.5 dpc, *Hes7* mRNA expression levels and transcription oscillate in wild-type (a-c, *n*=13/51 phase 1, 18/51 phase 2, 20/51 phase 3), *Lfng*$^{\Delta FCE1/\Delta FCE1}$ (d-f, *n*=13/32 phase 1, 8/32 phase 2, 11/32 phase 3) and *Lfng*$^{-/-}$ (g-i, *n*=10/22 phase 1, 5/22 phase 2, 7/22 phase 3) embryos. (**C**) *Hes7* RNA expression was examined using a cDNA probe that reveals the steady-state levels of mature *Hes7* mRNA. In wild-type 8.5 dpc embryos, several distinct patterns of expression are seen (a-c, *n*=9), while in *Lfng*$^{\Delta FCE1/\Delta FCE1}$ (d, *n*=7) embryos, *Hes7* mRNA is found ubiquitously throughout the PSM. At 10.5 dpc, oscillatory expression is seen in both wild-type (e, *n*=11; f, *n*=9) and *Lfng*$^{\Delta FCE1/\Delta FCE1}$ (g, *n*=8, h, *n*=9) embryos. (**D**) 10.5 dpc embryos were bisected along the neural tube, and one half was fixed (a,c,e), while the other half was cultured for 1 hour prior to fixation (b,d,f). The *Hes7* expression pattern is altered between the fixed and cultured halves of wild-type (a,b), *Lfng*$^{\Delta FCE1/\Delta FCE1}$ (c,d) and *Lfng*$^{-/-}$ (e,f) embryos, confirming that *Hes7* RNA levels can oscillate in the absence of LFNG activity.

pathway, although in zebrafish these segments can be affected by the simultaneous downregulation of several clock components (Oates et al., 2005) perhaps indicating multiple, parallel mechanisms of regulation. More recently, it has been shown that in zebrafish the anlagen of the anterior trunk, posterior trunk and tail are specified before somitogenesis begins, raising the possibility that different genetic pathways may affect these regions in distinct ways (Szeto and Kimelman, 2006).

Our data expand on these observations, suggesting that in the mouse, somite formation during secondary body formation is controlled largely by pathways that do not require oscillatory Notch1 activation. The robust nature of somitogenesis may reflect the existence of multiple, overlapping and interacting feedback loops controlling the oscillation of numerous genes in the Notch, Wnt and FGF pathways (Dequeant et al., 2006). For example, recent findings suggest that FGF signaling is required for oscillatory function of both the Notch and Wnt pathways in the PSM (Wahl et al., 2007), though most observations were confined to primary body formation. Our data support the additional hypothesis that oscillation of any individual pathway or component may be more or less important during different stages of somitogenesis. Our finding that *Hes7* oscillations recover during secondary body formation is especially interesting in light of recent findings that *Hes7* oscillations are regulated in part by the FGF pathway, and that oscillatory HES7 protein regulates the expression of FGF pathway components (Niwa et al., 2007). It is clear that regulated crosstalk among these pathways is important; however, our results suggest that specific interactions may be differentially regulated during primary and secondary body formation.

Wnt activity may play especially important roles in the regulation of posterior somitogenesis. Reductions in Wnt signaling levels can preferentially affect segmentation of the posterior embryo: the *Wnt3a*^{vt} hypomorphic allele develops segmentation defects in the lumbar, sacral and tail regions, and mutations in *Lrp6*, encoding a Wnt co-receptor, affect the caudal axial skeleton more severely than anterior skeletal regions (Kokubu et al., 2004; Pinson et al., 2000). These data may indicate that the caudal skeleton is more sensitive to perturbations in Wnt pathway activity. Conversely, based on our data, Notch oscillations may play a more important role during the development of the thoracic and lumbar skeleton. It will clearly be important to carefully dissect the interactions among these three pathways to clarify fully the possibility that the segmentation clock mechanism is differentially regulated during primary and secondary body formation.

R/C patterning of anterior somites may affect ongoing segmentation during secondary body formation

We find that many aspects of clock function recover in both *Lfng*$^{-/-}$ and *Lfng*$^{\Delta FCE1/\Delta FCE1}$ embryos after tailbud formation; however, the posterior skeletal phenotypes of *Lfng*$^{-/-}$ animals are much more

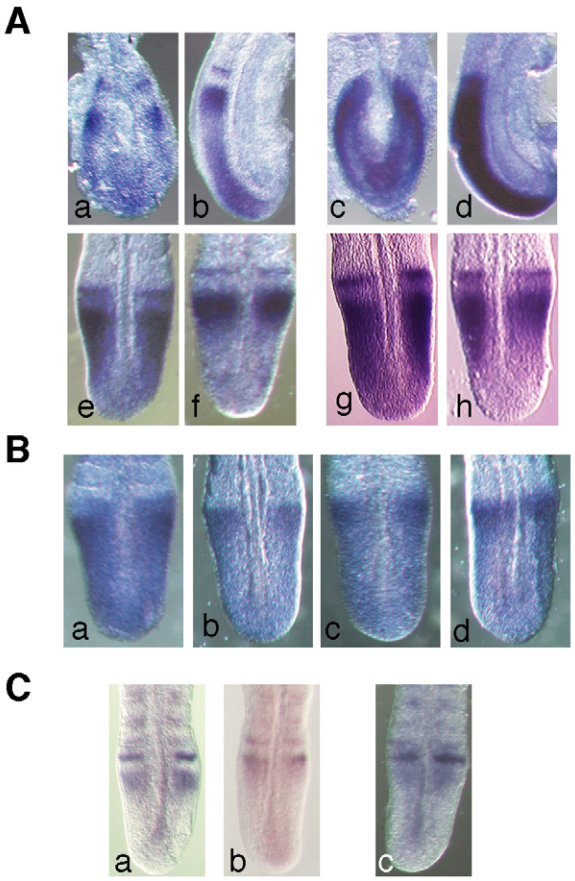

Fig. 7. Oscillatory gene expression is variously perturbed in *Lfng*$^{\Delta FCE1/\Delta FCE1}$ embryos. (**A**) *Nrarp* expression oscillates in wild-type embryos at 8.5 dpc (a,b, *n*=10), but is stably expressed in *Lfng*$^{\Delta FCE1/\Delta FCE1}$ embryos (c,d, *n*=6). At 10.5 dpc, wild-type embryos exhibit two distinct patterns of expression (e, *n*=7; f, *n*=8). Both these phases are seen in *Lfng*$^{\Delta FCE1/\Delta FCE1}$ embryos, but the pattern is more diffuse than that observed in wild-type embryos (g, *n*=5; h, *n*=2). (**B**) Cyclic expression of the *Dll1* intron probe is observed in both wild-type (a, *n*=6; b, *n*=7) and *Lfng*$^{\Delta FCE1/\Delta FCE1}$ (c, *n*=6; d, *n*=4) embryos at 10.5 dpc. (**C**) In wild-type embryos, two phases of *Hesr1* expression are seen, with a narrow band in the anterior PSM and either a broad (a, *n*=4) or narrow (b, *n*=2) band in the posterior PSM. *Hesr1* expression is perturbed in *Lfng*$^{\Delta FCE1/\Delta FCE1}$ embryos, with a diffuse band of staining extending from the posterior into the anterior PSM that overlies a narrow band of expression in the anterior PSM (c, *n*=6).

severe than those seen in *Lfng*$^{\Delta FCE1/\Delta FCE1}$ embryos. Therefore, we propose that the truncation of posterior skeletal structures in *Lfng*$^{-/-}$ animals is caused by the perturbation of R/C patterning in these embryos, rather than the loss of oscillatory Notch activity in the clock. Several lines of evidence suggest that R/C somite patterning contributes to the proper segmentation of the posterior embryo. Targeted deletion of *Mesp2*, which is exclusively expressed in region II of the PSM, causes disrupted R/C somite patterning and truncation of the posterior skeleton (Saga et al., 1997). Furthermore, it appears that the total dosage of MESP activity (comprising the additive effects of MESP1 and MESP2) in region II of the PSM is important. Manipulating the levels of MESP proteins can both partially rescue the R/C patterning of the somites and mitigate the caudal truncation of the axial skeleton (Morimoto et al., 2006). In addition, in newly developed *Mesp2* knockout alleles, *Mesp1* expression is elevated leading to partial rescue of somitogenesis during secondary body formation (Takahashi et al., 2007). Interestingly, an *Mesp2* mutation found in spondylocostal dysostosis also has more severe effects on the thoracic vertebrae than the more caudal skeleton (Whittock et al., 2004).

One possible explanation for these results is that continued R/C somite patterning is necessary for segmentation to proceed normally during secondary body formation. This could suggest that information transfer in the PSM can occur from the anterior to the tailbud, and that the segmentation of the most caudal embryonic structures may be reliant on proper patterning of more anterior structures. We propose that the expression of *Lfng* in the anterior PSM and the subsequent amelioration of R/C patterning defects in *Lfng*$^{\Delta FCE1/\Delta FCE1}$ embryos, permits posterior segmentation to proceed relatively normally, preventing the tail truncation seen in *Lfng*$^{-/-}$ animals. This underscores the potential for the transfer of information between the anterior and posterior regions of the PSM, at least during secondary body formation. Thus, the work reported here uncovers new levels of complexity linking differential regulation of clock function and R/C somite patterning to the long-known but little-understood processes of primary and secondary body formation.

We thank J. Thompson for critical reading of the manuscript, R. Johnson for *Lfng*^{tmRjo1} mice, and Y. Saga and P. Gruss for reagents. ES cell injections were performed by the OSUCCC ES cell core facility. This work was supported in part by Basil O'Connor grant #5-FY04-217 from the March of Dimes.

References

Aulehla, A. and Johnson, R. L. (1999). Dynamic expression of lunatic fringe suggests a link between notch signaling and an autonomous cellular oscillator driving somite segmentation. *Dev. Biol.* **207**, 49-61.

Aulehla, A., Wehrle, C., Brand-Saberi, B., Kemler, R., Gossler, A., Kanzler, B. and Herrmann, B. G. (2003). Wnt3a plays a major role in the segmentation clock controlling somitogenesis. *Dev. Cell* **4**, 395-406.

Bulman, M. P., Kusumi, K., Frayling, T. M., McKeown, C., Garrett, C., Lander, E. S., Krumlauf, R., Hattersley, A. T., Ellard, S. and Turnpenny, P. D. (2000). Mutations in the human delta homologue, DLL3, cause axial skeletal defects in spondylocostal dysostosis. *Nat. Genet.* **24**, 438-441.

Bunting, M., Bernstein, K. E., Greer, J. M., Capecchi, M. R. and Thomas, K. R. (1999). Targeting genes for self-excision in the germ line. *Genes Dev.* **13**, 1524-1528.

Candia, A. F., Hu, J., Crosby, J., Lalley, P. A., Noden, D., Nadeau, J. H. and Wright, C. V. (1992). Mox-1 and Mox-2 define a novel homeobox gene subfamily and are differentially expressed during early mesodermal patterning in mouse embryos. *Development* **116**, 1123-1136.

Chen, J., Kang, L. and Zhang, N. (2005). Negative feedback loop formed by Lunatic fringe and Hes7 controls their oscillatory expression during somitogenesis. *Genesis* **43**, 196-204.

Christ, B., Schmidt, C., Huang, R., Wilting, J. and Brand-Saberi, B. (1998). Segmentation of the vertebrate body. *Anat. Embryol.* **197**, 1-8.

Cole, S. E., Levorse, J. M., Tilghman, S. M. and Vogt, T. F. (2002). Clock regulatory elements control cyclic expression of Lunatic fringe during somitogenesis. *Dev. Cell* **3**, 75-84.

Cooke, J. and Zeeman, E. C. (1976). A clock and wavefront model for control of the number of repeated structures during animal morphogenesis. *J. Theor. Biol.* **58**, 455-476.

Dale, J. K., Maroto, M., Dequeant, M. L., Malapert, P., McGrew, M. and Pourquie, O. (2003). Periodic notch inhibition by lunatic fringe underlies the chick segmentation clock. *Nature* **421**, 275-278.

Deng, C., Wynshaw-Boris, A., Zhou, F., Kuo, A. and Leder, P. (1996). Fibroblast growth factor receptor 3 is a negative regulator of bone growth. *Cell* **84**, 911-921.

Dequeant, M. L., Glynn, E., Gaudenz, K., Wahl, M., Chen, J., Mushegian, A. and Pourquie, O. (2006). A complex oscillating network of signaling genes underlies the mouse segmentation clock. *Science* **314**, 1595-1598.

Dubrulle, J., McGrew, M. J. and Pourquie, O. (2001). FGF signaling controls somite boundary position and regulates segmentation clock control of spatiotemporal Hox gene activation. *Cell* **106**, 219-232.

Dunwoodie, S. L., Clements, M., Sparrow, D. B., Sa, X., Conlon, R. A. and Beddington, R. S. (2002). Axial skeletal defects caused by mutation in the spondylocostal dysplasia/pudgy gene Dll3 are associated with disruption of the

segmentation clock within the presomitic mesoderm. *Development* **129**, 1795-1806.
Evrard, Y. A., Lun, Y., Aulehla, A., Gan, L. and Johnson, R. L. (1998). *lunatic fringe* is an essential mediator of somite segmentation and patterning. *Nature* **394**, 377-381.
Forsberg, H., Crozet, F. and Brown, N. A. (1998). Waves of mouse Lunatic fringe expression, in four-hour cycles at two-hour intervals, precede somite boundary formation. *Curr. Biol.* **8**, 1027-1030.
Geffers, I., Serth, K., Chapman, G., Jaekel, R., Schuster-Gossler, K., Cordes, R., Sparrow, D. B., Kremmer, E., Dunwoodie, S. L., Klein, T. et al. (2007). Divergent functions and distinct localization of the Notch ligands DLL1 and DLL3 in vivo. *J. Cell Biol.* **178**, 465-476.
Gossler, A. and Tam, P. P. (2002). Somitogenesis: segmentation of the paraxial mesoderm and the delineation of tissue compartments. In *Mouse Development* (ed. J. Rossant and P. P. Tam), pp. 122-149. San Diego: Academic Press.
Gossler, A. and Hrabe de Angelis, M. (1998). Somitogenesis. *Curr. Top Dev. Biol.* **38**, 225-287.
Handrigan, G. R. (2003). Concordia discors: duality in the origin of the vertebrate tail. *J. Anat.* **202**, 255-267.
Holmdahl, D. E. (1925). Experimentelle Untersuchungen uber die Lage der Grenze zwischen primarer und sekundarere Korperentwicklung beim Huhn. *Anat. Anz.* **59**, 393-396.
Huppert, S. S., Ilagan, M. X., De Strooper, B. and Kopan, R. (2005). Analysis of Notch Function in presomitic mesoderm suggests a gamma-secretase-independent role for presenilins in somite differentiation. *Dev. Cell* **8**, 677-688.
Ishikawa, A., Kitajima, S., Takahashi, Y., Kokubo, H., Kanno, J., Inoue, T. and Saga, Y. (2004). Mouse Nkd1, a Wnt antagonist, exhibits oscillatory gene expression in the PSM under the control of Notch signaling. *Mech. Dev.* **121**, 1443-1453.
Johnston, S. H., Rauskolb, C., Wilson, R., Prabhakaran, B., Irvine, K. D. and Vogt, T. F. (1997). A family of mammalian Fringe genes implicated in boundary determination and the Notch pathway. *Development* **124**, 2245-2254.
Kerszberg, M. and Wolpert, L. (2000). A clock and trail model for somite formation, specialization and polarization. *J. Theor. Biol.* **205**, 505-510.
Kessel, M. and Gruss, P. (1991). Homeotic transformations of murine vertebrae and concomitant alteration of Hox codes induced by retinoic acid. *Cell* **67**, 89-104.
Kokubu, C., Heinzmann, U., Kokubu, T., Sakai, N., Kubota, T., Kawai, M., Wahl, M. B., Galceran, J., Grosschedl, R., Ozono, K. et al. (2004). Skeletal defects in ringelschwanz mutant mice reveal that Lrp6 is required for proper somitogenesis and osteogenesis. *Development* **131**, 5469-5480.
Kusumi, K., Mimoto, M. S., Covello, K. L., Beddington, R. S., Krumlauf, R. and Dunwoodie, S. L. (2004). Dll3 pudgy mutation differentially disrupts dynamic expression of somite genes. *Genesis* **39**, 115-121.
Mansouri, A., Yokota, Y., Wehr, R., Copeland, N. G., Jenkins, N. A. and Gruss, P. (1997). Paired-related murine homeobox gene expressed in the developing sclerotome, kidney, and nervous system. *Dev. Dyn.* **210**, 53-65.
McGrew, M. J., Dale, J. K., Fraboulet, S. and Pourquie, O. (1998). The lunatic fringe gene is a target of the molecular clock linked to somite segmentation in avian embryos. *Curr. Biol.* **8**, 979-982.
Meinhardt, H. (1986). Models of segmentation. In *Somites in Developing Embryos* (ed. R. Bellairs, D. A. Ede and J. W. Lash), pp. 179-189. New York: Plenum Press.
Morales, A. V., Yasuda, Y. and Ish-Horowicz, D. (2002). Periodic Lunatic fringe expression is controlled during segmentation by a cyclic transcriptional enhancer responsive to notch signaling. *Dev. Cell* **3**, 63-74.
Morimoto, M., Takahashi, Y., Endo, M. and Saga, Y. (2005). The Mesp2 transcription factor establishes segmental borders by suppressing Notch activity. *Nature* **435**, 354-359.
Morimoto, M., Kiso, M., Sasaki, N. and Saga, Y. (2006). Cooperative Mesp activity is required for normal somitogenesis along the anterior-posterior axis. *Dev. Biol.* **300**, 687-698.
Niwa, Y., Masamizu, Y., Liu, T., Nakayama, R., Deng, C. X. and Kageyama, R. (2007). The initiation and propagation of Hes7 oscillation are cooperatively regulated by Fgf and notch signaling in the somite segmentation clock. *Dev. Cell* **13**, 298-304.
Oates, A. C., Mueller, C. and Ho, R. K. (2005). Cooperative function of deltaC and her7 in anterior segment formation. *Dev. Biol.* **280**, 133-149.
Palmeirim, I., Henrique, D., Ish-Horowicz, D. and Pourquie, O. (1997). Avian hairy gene expression identifies a molecular clock linked to vertebrate segmentation and somitogenesis. *Cell* **91**, 639-648.
Pinson, K. I., Brennan, J., Monkley, S., Avery, B. J. and Skarnes, W. C. (2000). An LDL-receptor-related protein mediates Wnt signalling in mice. *Nature* **407**, 535-538.
Prince, V. E., Holley, S. A., Bally-Cuif, L., Prabhakaran, B., Oates, A. C., Ho, R. K. and Vogt, T. F. (2001). Zebrafish lunatic fringe demarcates segmental boundaries. *Mech. Dev.* **105**, 175-180.
Rida, P. C., Le Minh, N. and Jiang, Y. J. (2004). A Notch feeling of somite segmentation and beyond. *Dev. Biol.* **265**, 2-22.
Riddle, R. D., Johnson, R. L., Laufer, E. and Tabin, C. (1993). Sonic hedgehog mediates the polarizing activity of the ZPA. *Cell* **75**, 1401-1416.
Saga, Y. and Takeda, H. (2001). The making of the somite: molecular events in vertebrate segmentation. *Nat. Rev. Genet.* **2**, 835-845.
Saga, Y., Hata, N., Koseki, H. and Taketo, M. M. (1997). Mesp2: a novel mouse gene expressed in the presegmented mesoderm and essential for segmentation initiation. *Genes Dev.* **11**, 1827-1839.
Sawada, A., Shinya, M., Jiang, Y. J., Kawakami, A., Kuroiwa, A. and Takeda, H. (2001). Fgf/MAPK signalling is a crucial positional cue in somite boundary formation. *Development* **128**, 4873-4880.
Schnell, S. and Maini, P. K. (2000). Clock and induction model for somitogenesis. *Dev. Dyn.* **217**, 415-420.
Serth, K., Schuster-Gossler, K., Cordes, R. and Gossler, A. (2003). Transcriptional oscillation of lunatic fringe is essential for somitogenesis. *Genes Dev.* **17**, 912-925.
Shifley, E. T. and Cole, S. E. (2007). The vertebrate segmentation clock and its role in skeletal birth defects. *Birth Defects Res. C Embryo Today* **81**, 121-133.
Sparrow, D. B., Chapman, G., Wouters, M. A., Whittock, N. V., Ellard, S., Fatkin, D., Turnpenny, P. D., Kusumi, K., Sillence, D. and Dunwoodie, S. L. (2006). Mutation of the LUNATIC FRINGE gene in humans causes spondylocostal dysostosis with a severe vertebral phenotype. *Am. J. Hum. Genet.* **78**, 28-37.
Szeto, D. P. and Kimelman, D. (2006). The regulation of mesodermal progenitor cell commitment to somitogenesis subdivides the zebrafish body musculature into distinct domains. *Genes Dev.* **20**, 1923-1932.
Takahashi, Y., Koizumi, K., Takagi, A., Kitajima, S., Inoue, T., Koseki, H. and Saga, Y. (2000). Mesp2 initiates somite segmentation through the Notch signalling pathway. *Nat. Genet.* **25**, 390-396.
Takahashi, Y., Yasuhiko, Y., Kitajima, S., Kanno, J. and Saga, Y. (2007). Appropriate suppression of Notch signaling by Mesp factors is essential for stripe pattern formation leading to segment boundary formation. *Dev. Biol.* **304**, 593-603.
Truett, G. E., Heeger, P., Mynatt, R. L., Truett, A. A., Walker, J. A. and Warman, M. L. (2000). Preparation of PCR-quality mouse genomic DNA with hot sodium hydroxide and tris (HotSHOT). *Biotechniques* **29**, 52, 54.
Wahl, M. B., Deng, C., Lewandoski, M. and Pourquié, O. (2007). FGF signaling acts upstream of the NOTCH and WNT signaling pathways to control segmentation clock oscillations in mouse somitogenesis. *Development* **134**, 4033-4041.
Whittock, N. V., Sparrow, D. B., Wouters, M. A., Sillence, D., Ellard, S., Dunwoodie, S. L. and Turnpenny, P. D. (2004). Mutated MESP2 causes spondylocostal dysostosis in humans. *Am. J. Hum. Genet.* **74**, 1249-1254.
Zhang, N. and Gridley, T. (1998). Defects in somite formation in lunatic fringe-deficient mice. *Nature* **394**, 374-377.